

# Relationship Between the Parameters of Corneal and Fundus Pulse Signals Acquired With a Combined Ultrasound and Laser Interferometry Technique

Monika E. Danielewska<sup>1</sup>, Alina Messner<sup>2</sup>, René M. Werkmeister<sup>2</sup>, Michał M. Placek<sup>1</sup>, Valentin Aranha dos Santos<sup>2</sup>, Marek Rękas<sup>3</sup>, and Leopold Schmetterer<sup>2,4-7</sup>

<sup>1</sup> Wrocław University of Science and Technology, Department of Biomedical Engineering, Faculty of Fundamental Problems of Technology, Wrocław, Poland

<sup>2</sup> Center for Medical Physics and Biomedical Engineering, Medical University of Vienna, Vienna, Austria

<sup>3</sup> Department of Ophthalmology, Military Institute of Medicine, Warsaw, Poland

<sup>4</sup> Singapore Eye Research Institute, Singapore National Eye Centre, Singapore

<sup>5</sup> Academic Clinical Program, Duke-NUS Medical School, Singapore

<sup>6</sup> Department of Ophthalmology, Lee Kong Chian School of Medicine, Nanyang Technological University, Singapore

<sup>7</sup> Department of Clinical Pharmacology, Medical University of Vienna, Vienna, Austria

**Correspondence:** Monika E. Danielewska, Wrocław University of Science and Technology, Faculty of Fundamental Problems of Technology, Department of Biomedical Engineering, Wybrzeże Wyspiańskiego 27, 50-370 Wrocław, Poland. e-mail: monika.danielewska@pwr.edu.pl

**Received:** 10 February 2019

**Accepted:** 10 June 2019

**Published:** 1 August 2019

**Keywords:** ocular pulse; posterior/anterior eye system; spectral analysis

**Citation:** Danielewska ME, Messner A, Werkmeister RM, Placek MM, Aranha dos Santos V, Rękas M, Schmetterer L. Relationship between the parameters of corneal and fundus pulse signals acquired with a combined ultrasound and laser interferometry technique. *Trans Vis Sci Tech.* 2019;8(4):15. <https://doi.org/10.1167/tvst.8.4.15> Copyright 2019 The Authors

**Purpose:** To estimate the relationship between the characteristics of the corneal pulse (CP) signal and those of the fundus pulse (FP) signal measured with a combined noncontact ultrasonic and laser interferometry technique in healthy subjects.

**Methods:** Twenty-two healthy subjects participated in experiments that included measurements of intraocular pressure, ocular pulse amplitude, ocular biometry, blood pressure, and heart rate. Additionally, simultaneous recordings of CP and FP signals were acquired with a noncontact ultrasonic device combined with laser interferometry. Subsequently, ocular perfusion pressure (OPP) and the time and spectral parameters of CP and FP signals were computed. A system model was proposed to relate the FP signal to the CP signal.

**Results:** The system model revealed that the eye globe transfers information between signals of the posterior and anterior eye, relatively amplifying higher spectral harmonics. The amplitude of the second CP harmonic is predicted by  $FP_{RMS}$  and OPP ( $R^2 = 0.468$ ,  $P = 0.002$ ). Partial correlation analysis showed that the CP signal parameters are statistically significantly correlated with those of the FP signal and OPP, after correcting for age and sex.

**Conclusions:** The eye globe can be viewed as a *high pass filter*, in which the CP characteristic changes in relation to the fundus pulsation. The FP signal and OPP have an impact on the variations of the CP signal morphology.

**Translational Relevance:** Investigation of differences between the characteristics of the anterior and posterior tissue movements is a promising method for evaluating the role of circulatory and biomechanical components in the pathophysiology of ocular diseases.

## Introduction

The investigation of abnormalities in the eye pulsation has become of interest in ocular diseases such as glaucoma,<sup>1-5</sup> diabetic retinopathy,<sup>6,7</sup> and age-related macular degeneration,<sup>8,9</sup> as well as in systemic

diseases like carotid artery stenosis<sup>10,11</sup> and diabetes mellitus.<sup>12,13</sup> Recently, the measurement of eye pulsation has been employed for assessing the efficacy of glaucoma surgery.<sup>14</sup>

The dynamic movement of the eye's tissue originates from pulsatile changes of intraocular pressure (IOP), ocular, in particular choroidal,

hemodynamics, and aqueous humor dynamics.<sup>15,16</sup> This highly complex phenomenon, called the ocular pulse (OP), is in close relationship to cardiovascular activity.<sup>17-19</sup> The OP is characterized by ocular volume changes, which result in pulsatile displacements of the eye tissues, specifically those of cornea, sclera, and retina.<sup>3,20-23</sup> When measured with low-coherence tissue interferometry<sup>24</sup> or dynamic contour tonometry (DCT),<sup>25</sup> those displacements yield time series that, in general, can be referred to as OP signals. Characteristics of the measured OP signals have the potential to reveal both biomechanical and vascular components, as well as to serve as indicators for differentiating diseased eyes from healthy ones.<sup>1,3,5</sup> For example, analysis of the IOP pulse has shown the ability to distinguish healthy eyes from those of glaucoma suspects.<sup>26</sup> Reduced ocular pulse amplitude (OPA), measured with DCT, has been found in patients with normal-tension glaucoma (NTG) or primary open-angle glaucoma (POAG) when compared with the results of healthy individuals.<sup>5</sup> A low OPA has also been reported to correlate with moderate to severe glaucomatous visual field loss and has been suggested as an independent risk factor for visual field deterioration.<sup>27</sup> Also, reduction in pulsatile ocular blood flow (POBF) parameters have been found in eyes with glaucoma, in particular those with NTG,<sup>28</sup> pointing toward a role of POBF in the diagnosis of the disease.<sup>29</sup> Furthermore, the corneal pulse (CP) characteristic has been shown to carry, in an indirect way, information about both, IOP variations and changes in corneal biomechanics after canaloplasty (Danielewska ME, et al. *IOVS*. 2018;59:ARVO E-Abstract 2022; Danielewska ME, et al. *IOVS*. 2019;60:ARVO E-Abstract 6202).

Although many of the OP measurement techniques require contact with the ocular surface, others enable noncontact, in vivo OP measurement. In particular, laser and low-coherence interferometry<sup>20,24,30,31</sup> and Fourier-domain optical coherence tomography (OCT)<sup>23,32</sup> were proposed to register OP. The latter has been used for noninvasive and simultaneous measurement of the movements of cornea and retina. The fundus pulse (FP) was then assessed simply as the difference between the two movements. Video recording and air-coupled ultrasonic micro-displacement measurement technology have also been used to measure longitudinal corneal displacements.<sup>21,22,33</sup> Furthermore, combining the ultrasound technique for assessment of corneal movement with spectral- and time-domain OCT, a synchronous measurement of corneal displacement in one eye and an evaluation

of retinal blood flow in the contralateral eye, have been performed (Danielewska ME, et al. *IOVS*. 2012;53:ARVO E-Abstract 5649). Nonetheless, no information has yet been obtained on the relationship between displacement signals of the retina and those of the cornea. Hence, further investigation of such a relationship using a noncontact technique can provide more insight into eye dynamics and offer additional diagnostic indicators with physiological and clinical utility in ocular diseases, such as glaucoma.

In the current study, we aimed at assessing the relationship between the parameters of CP and FP signals acquired with a technique that combines ultrasonic micro-displacement measurement technology with laser interferometry in a group of healthy individuals, using methods of time and spectral analysis.

## Methods

### Participants

The study was approved by the Bioethics Committee of the Military Institute of Medicine in Warsaw (decision No. 68/WIM/2015) and adhered to the tenets of the Declaration of Helsinki. The rationale of the study and the protocol were explained to the participants. Afterwards, written informed consent was obtained from all individuals.

Twenty-two left eyes of 22 healthy subjects were included in this study. All participants underwent general medical history review and standard ophthalmic examination including slit-lamp biomicroscopy and indirect funduscopy. Before CP and FP measurements, eye biometry (anterior chamber depth [ACD] and axial length [AL]) was measured using an optical biometry system (IOLMaster; Carl Zeiss Meditec AG, Jena, Germany), refraction was examined with an automatic Refracto-Keratometer (VISUREF 100; Carl Zeiss Meditec AG), and systolic blood pressure (SBP), diastolic blood pressure (DBP), and mean arterial pressure (MAP), as well as heart rate (HR) were measured on the upper arm with an automated oscillometric device (Infinity Delta monitor, Draeger Austria GmbH, Vienna, Austria). IOP and OPA were measured with the Pascal DCT (Swiss Microtechnology AG, Port, Switzerland), and central corneal thickness (CCT) was measured with an ultrasonic pachymeter (Handy Pachymeter SP-100, Tomey Corporation, Nagoya, Japan), after CP and FP measurement to avoid the influence of administering anesthetics to the anterior eye surface. Exclusion

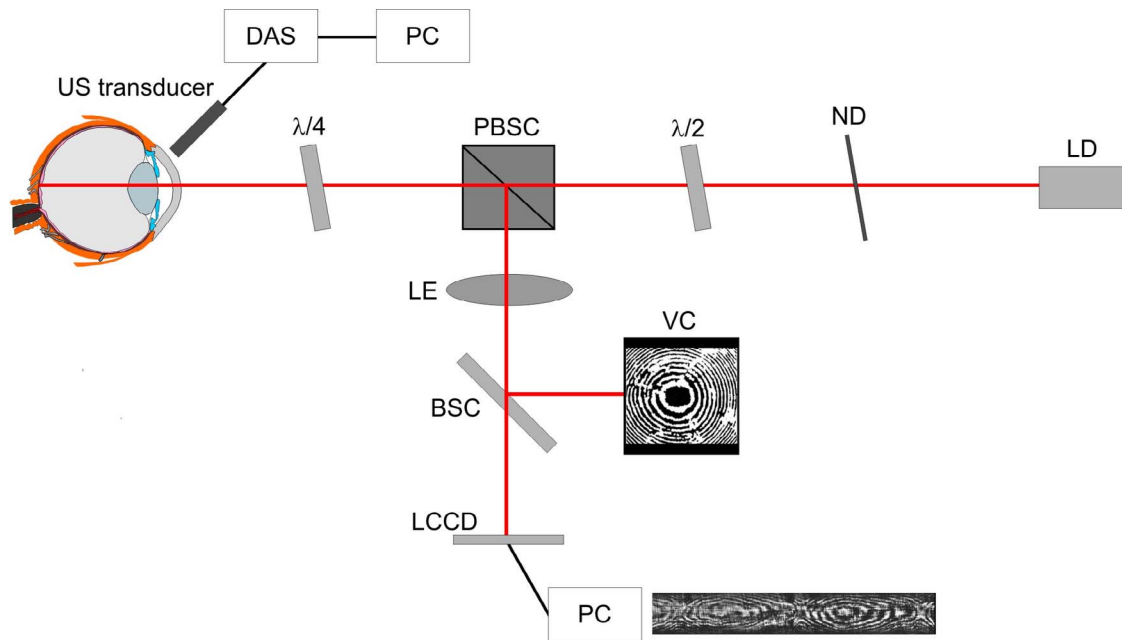


**Figure 1.** The scheme of measurements setup for simultaneous recording of the CP and FP signals using a noncontact ultrasonic (US) micro-displacement measurement technology combined with laser interferometry. DAS, data acquisition system; PC, computer;  $\lambda/4$  and  $\lambda/2$ , half- and quarter-wave plates; PBSC, polarizing beamsplitter cube; ND, neutral-density filter; LD, laser diode; LE, lens; BSC, beamsplitter cube; VC, video camera; LCCD, linear CCD array.

criteria were systemic diseases, any previous ocular surgical procedure, conjunctival or intraocular inflammation, and corneal abnormalities such as edema or scars.

### CP and FP Measurements

In this study, for the first time, a noncontact ultrasonic technique for registering the CP signal<sup>22,34</sup> and a laser interferometric method for recording the FP signal<sup>6,8,20</sup> were combined.

The measurement of the fundus pulsations is based on a laser interferometric method using a laser diode with a central wavelength of 780 nm and a long coherence length. The subject's eye is illuminated by the collimated laser beam (see Fig. 1). Part of the impinging light is reflected at the front surface of the cornea, another part at the ocular fundus, mainly at the retinal pigment epithelium or Bruch's membrane. The two reflected waves, a plane wave arising from the fundus and a spherical wave originating from the corneal surface interfere and generate concentric circular interference fringes in a plane several millimeters in front of the eye. These interference fringes are imaged onto a linear charge-coupled device (CCD) array. The rhythmic filling of ocular vessels during the cardiac cycle leads to a change in corneo-retinal distance. During the systole, distance

decreases, because the blood volume entering the eye via the arteries exceeds the blood volume leaving the eye via the veins, causing a slight protrusion of the retinal structures toward the cornea. During diastole, on the other hand, the distance between the two structures increases again. The maximum distance change during the cardiac cycle is called fundus pulsation amplitude (FPA). It is in the order of several micrometers and a measure for the pulsatile component of ocular blood flow during the cardiac cycle. These periodic changes lead to an in- and outward movement of the interference fringes that are recorded by the CCD array over time, resulting in a so-called synthetic interferogram. The latter thus covers information on the time course of changes in corneo-retinal distance and, by counting the fringes moving inward or outward and considering the wavelength of the light source, allows for determination of the FPA. In the current system, the FP signal was recorded using a CCD camera with 2048 pixels operated at a line readout rate of 450 Hz.

The power of the probe beam at the corneal front surface was approximately 80  $\mu\text{W}$ , well below the maximum permissible exposure, as specified by the safety standards (ANSI Z136.1-2014<sup>35</sup>; IEC 60825-1:2014<sup>36</sup>) to ensure ocular safety.

The probe beam of the interferometric method

illuminates the patient's eye centrally along the vision axis. The ultrasonic transducer for measurement of the corneal pulsations was therefore placed toward the peripheral cornea, mounted in a specially constructed holder and placed on a rigid platform stabilizing the device. In that case, the angle between the transducer axis and the direction of the beam of the FP measurement device was approximately  $60^\circ$ . Nonetheless, due to ocular surface expansion,<sup>22</sup> amplitude of the corneal normal displacements at its peripheral area appear to be similar to that at its central area. Details about the ultrasonic transducer were described in previous papers.<sup>22,34</sup> An adjustable headband and two holders were used to stabilize the head. Synchronized with the CP signal, measurements of the blood pulse (BPL) were performed using a pulse oximeter placed on the left earlobe. The simultaneous, but not synchronous, measurement of the CP and FP signals took 10 seconds and was repeated three times in each subject. During that time, the subject was asked to abstain from blinking and fixate on the 670 nm laser beam, which appears as a small red spot. In the CP recording, the sampling frequency was set to 400 Hz. The scheme of measurement setup is presented in [Figure 1](#).

## Data Analysis

Numerical signal analysis was performed in a custom program written in MATLAB (MathWorks, Natick, MA). First, the FP signals were interpolated to the sampling frequency of the CP and BPL signals. Then, all signals were filtered in the range from 0.5 to 20 Hz using an ideal bandpass filter.<sup>4</sup> This resulted in signal mean value, corresponding to the zero frequency, being removed. In the time-domain, the root mean squared (RMS) values of CP and FP signals were computed. The RMS value is a more appropriate measure than the signal amplitude for signals that are multicomponent or that have a structure more complicated than a simple sine wave. This is because RMS describes the square root of the overall signal energy, whereas the amplitude describes only the signal value at a given time instant.

Spectral analysis included calculation of the amplitude spectrum for all analyzed signals using the Fourier transform. Parameters such as frequencies of the first three harmonics related to the HR and their amplitudes were considered. Based on the BPL amplitude spectrum, the frequency of the first harmonic associated with the HR ( $f_{BPL1}$ ) was estimated. An assumption has been made that the BPL signal is stationary in the wide sense.<sup>18</sup> The

corresponding harmonics,  $f_{CP1}$ ,  $f_{FP1}$ , and their amplitudes,  $A_{CP1}$ ,  $A_{FP1}$ , in the CP and FP signals, respectively, were found. Then, the next two higher harmonics and their amplitudes,  $A_{CP2}$ ,  $A_{CP3}$ ,  $A_{FP2}$ ,  $A_{FP3}$ , were identified. Finally, for each subject, the mean values of all amplitudes across CP and FP signals were calculated from three repeated measurements.

For each subject, ocular perfusion pressure (OPP) was calculated as  $OPP = 2/3 (MAP - IOP)$ , where MAP and IOP are the mean values from the three repeated measurements.<sup>37</sup>

## Linear Time-Invariant (LTI) Model

To represent the relationship between FP and CP signals, a LTI system was designed. The identification of the LTI system was undertaken assuming the FP and CP signal as its input and output, respectively, and is given by,

$$S_{CP}(f) = S_{FP}(f)|H(f)|^2,$$

where  $S_{CP}(f)$  and  $S_{FP}(f)$  are the power spectral densities of the CP and FP signals, respectively, and  $H(f)$  is the transfer function of the LTI system. Note that in the equation above it was assumed that both FP and CP may contain random components. Consequently, the modulus of the transfer function was estimated using

$$|H(f)| = \sqrt{\frac{S_{CP}(f)}{S_{FP}(f)}}, S_{FP}(f) \neq 0.$$

$|H(f)|$  was calculated for each recording individually and then averaged over the recordings belonging to a particular subject (mean modulus of the transfer function  $|\bar{H}(f)|$ ).

## Statistical Analysis

Since the data were characterized by a statistically significant skewness at a significance level of  $\alpha = 0.05$ , a logarithmic transformation was applied. The  $t$ -test was used to compare the averaged amplitudes of the first three harmonics pair-wise, separately for the CP and FP signals. Following Armstrong,<sup>38</sup> no correction for multiple comparisons was applied.

To assess the relationships between temporal and spectral parameters of the CP signal and those of the FP signal, blood pressure (BP), and OPP, partial correlations were performed. Subject's age, sex, and HR were used as the control variables. Choosing age as a control variable was motivated by previous



studies showing that age is an important factor affecting the ocular blood flow,<sup>39,40</sup> in particular the choroidal blood flow reflected in reduced FP amplitude.<sup>35</sup> Sex-related differences in ocular blood flow are rarely considered; however, sex and hormonal status were shown to influence choroidal circulation.<sup>41,42</sup> The choice of HR as another control variable was motivated by the fact that changes in this parameter were found to affect the POBF.<sup>17</sup>

Further, to ascertain whether some of the FP signal parameters, OPP or other ocular parameters play a significant role in the CP signal parameter estimates, backward stepwise regression analysis was used with the following predictors:  $FP_{RMS}$ ,  $A_{FP1}$ ,  $A_{FP2}$ ,  $A_{FP3}$ , OPP, or ocular parameters (CCT, ACD, and AL). Calculations were performed in SPSS 22.0 (SPSS, Inc., Chicago, IL).

## Results

Fifteen female and seven male subjects aged from 21 to 58 ( $32 \pm 10$  years, mean  $\pm$  SD) were included. Demographic data, ocular and BP parameters are summarized in Table 1, whereas their distributions are shown in Figure 2.

Examples of time and frequency representations of CP, FP, and BPL signals for one subject are presented in Figure 3. In all the spectra, frequency components associated with the fundamental frequency of the heartbeat are observed. For better visualization of similarities between the spectral content of the three signals, the first three harmonics (i.e., the fundamental, the second, and the third harmonic) corresponding to the heartbeat are shown in Figure 3B. Comparing the position of the harmonics in the CP, FP, and BPL signal spectra, no frequency shifts between them were found.

Figure 4 presents averaged amplitudes of the first three harmonics of the CP and FP signals across all subjects. The second harmonic is the dominant frequency component in the CP signal and was found to be statistically significantly different from the first harmonic (paired  $t$ -test,  $P = 0.009$ ). However, the FP signal reveals a different spectral distribution, with the first harmonic being dominant and significantly different from the other two harmonics (paired  $t$ -tests, both  $P < 0.001$ ).

Results of the average modulus of transfer function  $|\bar{H}(f)|$  for each subject together with the group-averaged modulus of the transfer function and its 95% confidence interval is presented in Figure 5 for dimensionless frequency normalized to the funda-

**Table 1.** Patients' Demographics and the Considered Set of Parameters for All Subjects

Data	Mean $\pm$ SD	Range
Age (y)		
Total	$32 \pm 10$	21 to 58
Female	$32 \pm 10$	21 to 53
Male	$33 \pm 11$	26 to 58
CCT ( $\mu\text{m}$ )	$542 \pm 41$	458 to 625
ACD (mm)	$3.45 \pm 0.56$	1.90 to 4.45
AL (mm)	$23.82 \pm 1.31$	21.03 to 26.84
Spherical equivalent (D)	$-1.13 \pm 2.73$	-8.75 to 2.5
IOP (mm Hg)	$15.6 \pm 1.8$	12.1 to 18.7
OPA (mm Hg)	$3.0 \pm 1.2$	0.9 to 5.3
$CP_{RMS}$ ( $\mu\text{m}$ )	$18.6 \pm 6.5$	11.6 to 36.9
$A_{CP1}$ ( $\mu\text{m}$ )	$3.1 \pm 1.1$	1.6 to 5.7
$A_{CP2}$ ( $\mu\text{m}$ )	$4.7 \pm 2.7$	1.0 to 9.8
$A_{CP3}$ ( $\mu\text{m}$ )	$3.1 \pm 2.9$	0.9 to 13.4
FPA ( $\mu\text{m}$ )	$4 \pm 2$	2 to 7
$FP_{RMS}$ ( $\mu\text{m}$ )	$1.4 \pm 0.6$	0.6 to 2.6
$A_{FP1}$ ( $\mu\text{m}$ )	$0.5 \pm 0.3$	0.3 to 1.1
$A_{FP2}$ ( $\mu\text{m}$ )	$0.19 \pm 0.09$	0.08 to 0.34
$A_{FP3}$ ( $\mu\text{m}$ )	$0.09 \pm 0.06$	0.03 to 0.22
SBP (mm Hg)	$124 \pm 12$	103 to 155
DBP (mm Hg)	$76 \pm 10$	49 to 90
MAP (mm Hg)	$95 \pm 10$	77 to 111
OPP (mm Hg)	$80 \pm 11$	63 to 99
HR (beat/min)	$71 \pm 14$	34 to 102

mental frequency of the subject's HR. The eye globe can be viewed as a filter, which transmits higher frequencies (above 1 Hz) of the CP signal in relation to the FP signal. The effect of high-pass filtering is visible in each subject.

Table 2 contains the results of partial correlations between time (and spectral) parameters of the CP and the FP signals, BP, IOP, and OPP, with age, sex, and HR as the covariate variables. A statistically significant correlation of  $CP_{RMS}$  and  $A_{CP2}$  with parameters of the FP signal, BP, and OPP was found after correcting for age and sex.

In the backward stepwise regression analysis, there were no other parameters than  $FP_{RMS}$ ,  $A_{FP2}$ ,  $A_{FP3}$ , and OPP that had a statistically significant contribution to the estimation of the CP time and spectral parameters. Hence, only these predictors are presented. The statistically significant results of the linear regression models for prediction of  $CP_{RMS}$ ,  $A_{CP2}$ , and  $A_{CP3}$  are given in Table 3 and in Figure 6. Interestingly,  $FP_{RMS}$  and OPP as well as  $A_{FP2}$  and

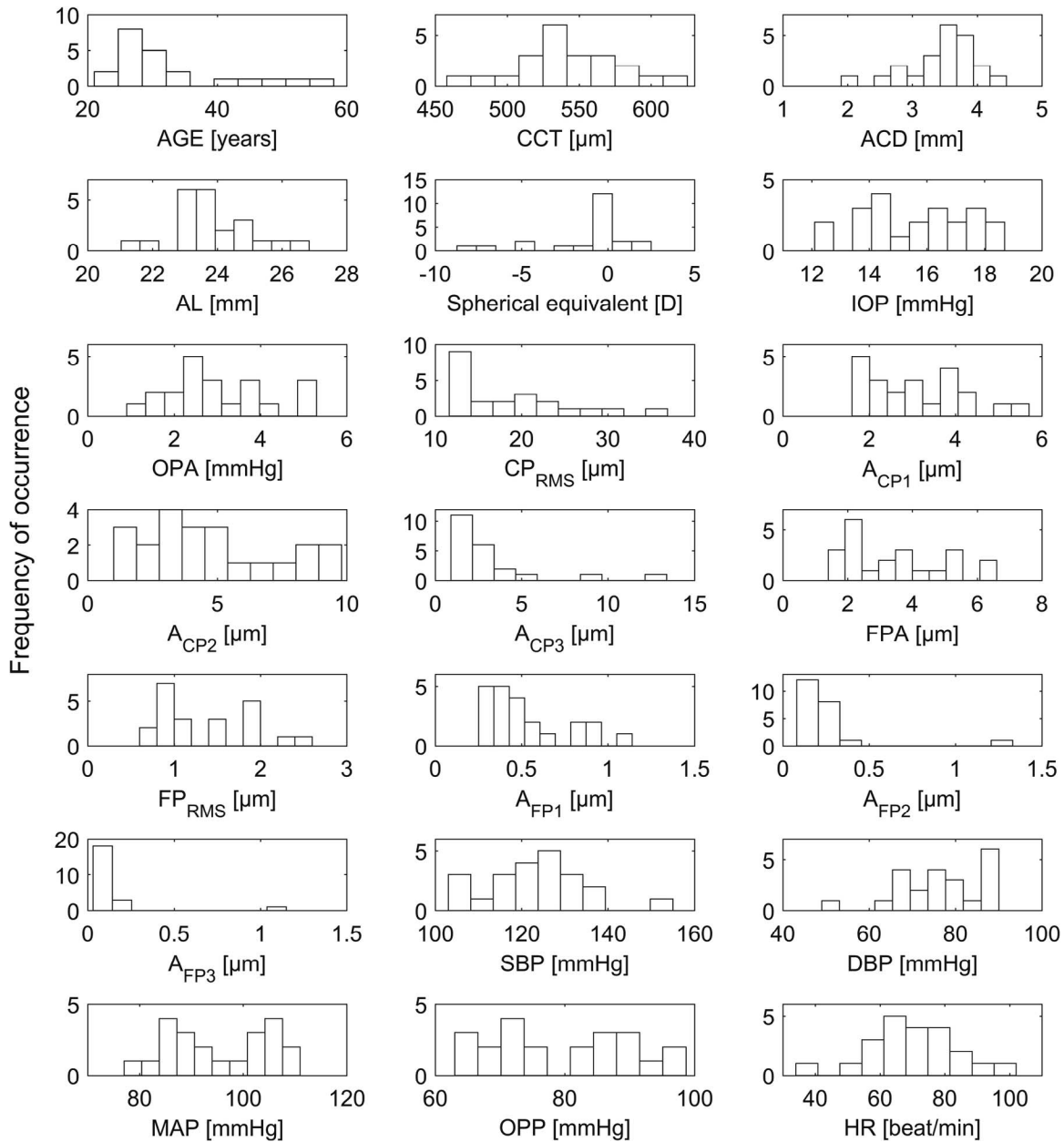


**Figure 2.** Distribution of the demographic data and ocular and BP parameters for all subjects.

$A_{FP3}$  are the predictors for amplitudes of the higher CP harmonics,  $A_{CP2}$  and  $A_{CP3}$ , respectively.

## Discussion

Techniques for noncontact, continuous, and simultaneous in vivo measurements of the natural movements of eye tissues during the cardiac cycle are valuable in the diagnosis of ocular diseases related to changes in ocular vasculature and/or biomechanics of ocular tissues.<sup>3,4,6</sup> Our study presents, for the first

time, an approach that combines ultrasonic micro-displacement measurement technology with laser interferometry in a group of healthy individuals. The findings complement the existing knowledge about the relationships between parameters of the CP signal and those of the FP signal during the cardiac cycle.

Given that the CP and FP signals are multicomponent, time and spectral analyses were applied to extract the parameters representing characteristic features of these signals. In general, spectral analyses

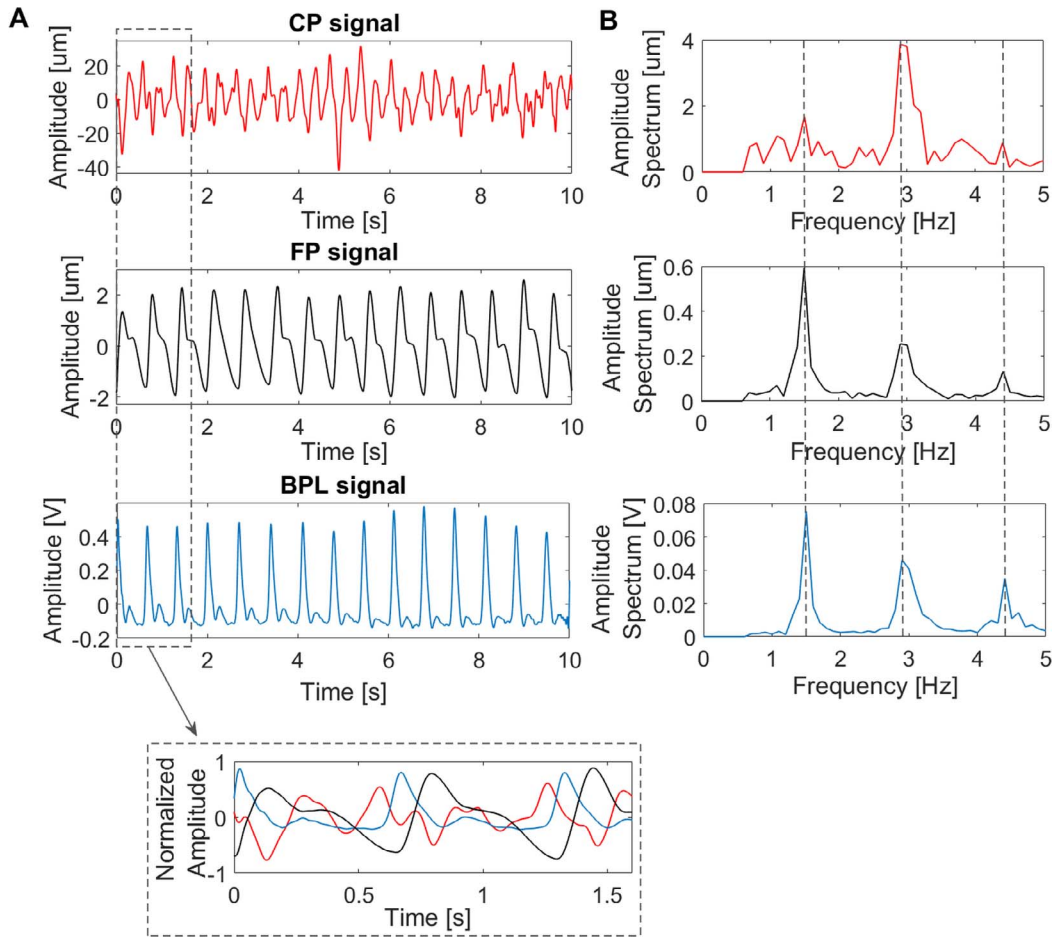


**Figure 3.** Illustrative time (A) and frequency (B) characteristics for the CP, FP, and BPL signals in the case of a 32-year-old female subject.

of the OP signals have been shown to be a powerful tool in many studies. To distinguish healthy subjects from those with glaucoma, spectral contents of the IOP pulse have been examined.<sup>1,26,43</sup> Amplitudes of

higher harmonics (the second, third, and fourth) of the IOP waveform for healthy and glaucomatous eyes have been found to be statistically significantly different between those two groups.<sup>1,43</sup> Spectral decomposition of pulsatile retinal movements, as a measure for the response of retinal and optic nerve head tissues to the cardiac pulsation, has demonstrated distinctive features between younger and older subjects, and those with glaucoma.<sup>3</sup> Dion et al.<sup>3</sup> noted that age-related and glaucomatous differences in the retinal pulse waveform can be linked to changes in the biomechanical properties of eye tissues corresponding to higher ocular rigidity. In our study, in healthy subjects, the considered LTI system with the FP signal being the input and the CP signal being the output of the system, revealed characteristic behaviors for the different harmonic frequencies related to the heartbeat. An amplitude of the first harmonic (fundamental frequency) contained in FP and CP spectra is damped by the eye globe, whereas amplitudes of the higher harmonics (second and third) are relatively

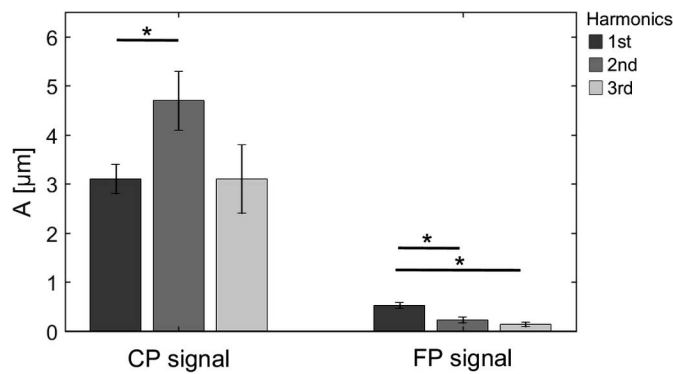


**Figure 4.** Amplitudes of the first three harmonics related to the heartbeat for CP and FP signals in all subjects. Results are represented as mean  $\pm$  standard error of the mean (SEM). \* Indicates  $P < 0.05$ .

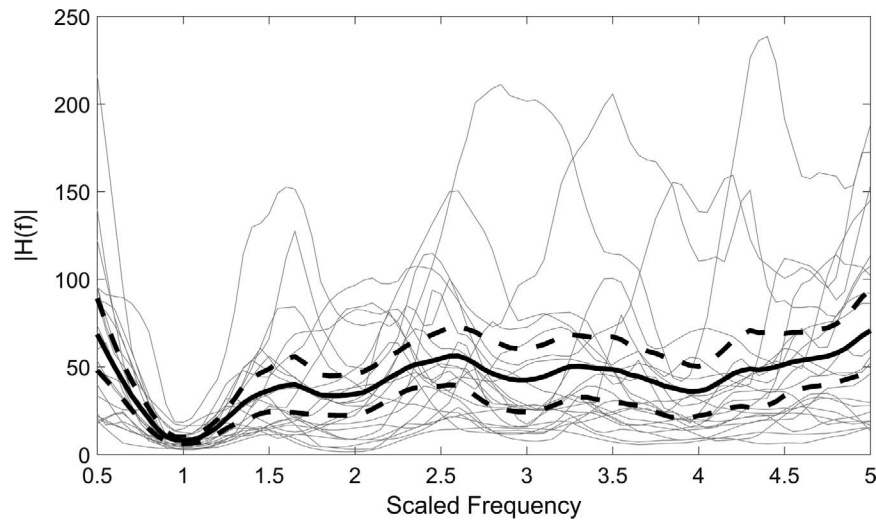


**Figure 5.** Transfer function  $|\bar{H}(f)|$  for each subject based on three realizations of the input-output signals (gray thin lines), group-averaged modulus of the transfer function (solid black line), and its 95% confidence interval (dashed black lines).

amplified. This result clearly shows that the eye globe system can be described as a *high pass filter* with a cut-off frequency of approximately 1 Hz (see Fig. 5), where the CP characteristics change in relation to the fundus pulsation.

The group average amplitudes of the considered harmonics of the CP and FP signals are in agreement with the results for healthy subjects reported by Singh et al.<sup>23</sup> These authors reported that the dominant harmonic in the FP signal is the first one, which corresponds to the fundamental frequency of the heartbeat, whereas in the CP signal, being more intricate than the FP signal, the dominant harmonic is the second one. The measurement setting used in these experiments was different to the one reported here. The difference between the characteristics of the anterior and the posterior tissue movements can be a valid natural phenomenon determining the correct visual process,<sup>44</sup> in which the vibrations of the optical components of the eye could have a beneficial aspect in terms of quality of vision.<sup>45</sup>

The temporal and spectral characteristics of the CP and FP signals can also be linked to different factors influencing the pulsation of the anterior and posterior eye tissues. Fundus pulsations were shown to be a valid index of pulsatile choroidal perfusion and are considered to be closely related to choroidal engorgement during the systole.<sup>46</sup> The behavior of the anterior eye is much more complicated. The cornea response changes according to, for example, BP wave propagation, IOP fluctuations, aqueous humor dynamics, and tissues biomechanics.<sup>16,18,21,22,47</sup> Recently, ocular volume changes measured with a

Triggerfish contact lens sensor (SENSIMED Triggerfish; Sensimed, Lausanne, Switzerland) were also shown to contribute to the anterior eye dynamics.<sup>14</sup> In the current study, we show that the CP signal, measured with the ultrasonic method at the peripheral cornea, does not necessarily share the characteristics of the retinal movements registered axially with the interferometric method. Otherwise, the correlation between the CP signal parameters and those of the fundus pulsation would likely be very strong. Hence, the CP signal may contain additional information about corneal surface expansion and its biomechanics.<sup>47</sup>

The dominance of the second harmonic in the CP signal, that is usually not observable with contact techniques such as DCT, may be explained by the biomechanical properties of the cornea and other ocular tissues. It has been reported that higher power of the third CP harmonic correlates with higher corneal stiffness (a higher Young's modulus), whereas the first CP harmonic correlates positively with the corresponding harmonic of the BPL signal related to the HR.<sup>47</sup> Changes in scleral stiffness can also have an impact on the characteristic of OP signals and, in consequence, on the corneal response (Roberts CJ, et al. *IOVS*. 2019;60:ARVO E-Abstract 4780),<sup>2</sup> because the sclera constantly undergoes IOP-related deformations. Further, biomechanics of other ocular tissues vary under mechanical stress, as they are a critical regulator of alterations in cell functions and structural properties.<sup>48,49</sup> For example, the conventional outflow pathway can have a direct effect on the corneal behavior, where related tissues are continuously



**Table 2.** Results of Partial Correlation Analysis Between Time (and Spectral) Parameters of the CP and the FP Signals, BP, and IOP, Controlling for Age, Sex, and HR

Parameters	FP <sub>RMS</sub>	A <sub>FP1</sub>	A <sub>FP2</sub>	A <sub>FP3</sub>	IOP	SBP	DBP	MAP	OPP
Age									
CP <sub>RMS</sub>									
<i>r</i>	-0.379	-0.322	-0.397	-0.295	<b>-0.626</b>	<b>0.459</b>	0.382	<b>0.449</b>	<b>0.516</b>
<i>P</i>	0.091	0.154	0.075	0.194	<b>0.002</b>	<b>0.036</b>	0.088	<b>0.041</b>	<b>0.017</b>
A <sub>CP1</sub>									
<i>r</i>	0.039	0.223	-0.006	0.051	-0.380	<b>0.490</b>	0.303	0.367	0.400
<i>P</i>	0.868	0.332	0.979	0.826	0.089	<b>0.024</b>	0.181	0.102	0.072
A <sub>CP2</sub>									
<i>r</i>	<b>-0.533</b>	-0.378	<b>-0.463</b>	<b>-0.435</b>	-0.365	0.390	<b>0.495</b>	<b>0.509</b>	<b>0.529</b>
<i>P</i>	<b>0.013</b>	0.091	<b>0.034</b>	<b>0.049</b>	0.104	0.081	<b>0.023</b>	<b>0.019</b>	<b>0.014</b>
A <sub>CP3</sub>									
<i>r</i>	0.181	0.044	0.152	0.351	-0.244	0.014	-0.178	-0.042	0.000
<i>P</i>	0.432	0.851	0.511	0.119	0.287	0.953	0.441	0.857	0.998
Sex									
CP <sub>RMS</sub>									
<i>r</i>	-0.429	-0.395	<b>-0.530</b>	<b>-0.511</b>	<b>-0.722</b>	0.392	0.394	<b>0.444</b>	<b>0.535</b>
<i>P</i>	0.053	0.076	<b>0.013</b>	<b>0.018</b>	<b>&lt; 0.001</b>	0.079	0.077	<b>0.044</b>	<b>0.012</b>
A <sub>CP1</sub>									
<i>r</i>	-0.018	0.179	-0.127	-0.140	<b>-0.467</b>	0.417	0.323	0.360	0.413
<i>P</i>	0.939	0.439	0.584	0.545	<b>0.033</b>	0.060	0.154	0.109	0.062
A <sub>CP2</sub>									
<i>r</i>	<b>-0.581</b>	<b>-0.439</b>	<b>-0.553</b>	<b>-0.571</b>	<b>-0.440</b>	0.400	0.424	<b>0.471</b>	<b>0.512</b>
<i>P</i>	<b>0.006</b>	<b>0.046</b>	<b>0.009</b>	<b>0.007</b>	<b>0.046</b>	0.073	0.055	<b>0.031</b>	<b>0.018</b>
A <sub>CP3</sub>									
<i>r</i>	0.138	-0.010	0.018	0.152	-0.364	-0.193	-0.200	-0.111	-0.040
<i>P</i>	0.550	0.965	0.938	0.511	0.105	0.402	0.386	0.633	0.864
HR									
CP <sub>RMS</sub>									
<i>r</i>	-0.380	-0.275	-0.400	-0.314	<b>-0.600</b>	<b>0.498</b>	0.348	0.395	<b>0.478</b>
<i>P</i>	0.109	0.254	0.090	0.190	<b>0.007</b>	<b>0.030</b>	0.144	0.094	<b>0.039</b>
A <sub>CP1</sub>									
<i>r</i>	-0.040	0.211	-0.084	-0.038	-0.375	<b>0.561</b>	0.378	0.420	<b>0.458</b>
<i>P</i>	0.871	0.386	0.734	0.878	0.114	<b>0.013</b>	0.111	0.073	<b>0.048</b>
A <sub>CP2</sub>									
<i>r</i>	<b>-0.475</b>	-0.315	-0.428	-0.351	-0.364	<b>0.506</b>	0.303	0.410	0.447
<i>P</i>	<b>0.040</b>	0.189	0.067	0.141	0.126	<b>0.027</b>	0.207	0.081	0.055
A <sub>CP3</sub>									
<i>r</i>	-0.126	-0.115	-0.062	0.074	-0.386	-0.011	-0.011	0.028	0.099
<i>P</i>	0.607	0.639	0.802	0.764	0.102	0.963	0.964	0.909	0.688

Bolded values indicate  $P < 0.05$ .

exposed to a dynamic stressor like IOP fluctuations.<sup>50</sup> The value of the IOP depends mainly on the balance between aqueous humor secretion<sup>51</sup> and aqueous humor outflow,<sup>52</sup> where the first is ciliary blood flow independent above a critical level of perfusion and

blood flow dependent below it.<sup>53</sup> A decrease in outflow facility has been reported as an active response of outflow tissues to the cyclic biomechanical stress<sup>16</sup> and has been suggested to be directly linked to an increased resistance through this

**Table 3.** Results of Backward Stepwise Regression Analysis for Predictors ( $FP_{RMS}$ ,  $A_{FP2}$ ,  $A_{FP3}$ , and  $OPP$ ) Contributing Statistically Significantly to the Estimation of the CP Time and Spectral Parameters ( $CP_{RMS}$ ,  $A_{CP2}$ , and  $A_{CP3}$ )

Model	Unstandardized Coefficients		Standardized Coefficients	$t$	$P$ Value	$R^2$	$F$	$P$ Value
	B	SE	$\beta$					
$CP_{RMS}$								
Constant	0.734	0.194	—	3.783	0.001	0.262	7.119	<b>0.015</b>
OPP	0.006	0.002	0.512	2.668	0.015			
$A_{CP2}$								
Constant	0.177	3.906	—	0.045	0.964	0.468	8.363	<b>0.002</b>
$FP_{RMS}$	-2.254	0.834	-0.468	-2.702	0.014			
OPP	0.096	0.043	0.391	2.256	0.036			
$A_{CP3}$								
Constant	0.471	0.150	—	3.145	0.005	0.312	4.301	<b>0.029</b>
$A_{FP2}$	-4.755	1.910	-1.348	-2.489	0.022			
$A_{FP3}$	8.659	3.011	1.557	2.876	0.010			

pathway. The resistance of the trabecular outflow pathways against the flow of the aqueous humor has a strong effect on IOP generation and consequently can influence the characteristic of the corneal pulsation.

Higher amplitudes of the second and third harmonics of the CP signal are responsible for formation of ocular dicrotism, a phenomenon ob-

served in elderly subjects<sup>54</sup> and even more frequently in glaucoma patients.<sup>4</sup> Ocular dicrotism is characterized by specific changes in the morphology of the CP signal, leading to the appearance of two distinct, sufficiently separated maxima during one heart cycle. The exact mechanism behind the formation of the ocular dicrotic pulse (ODP) signal has not been fully

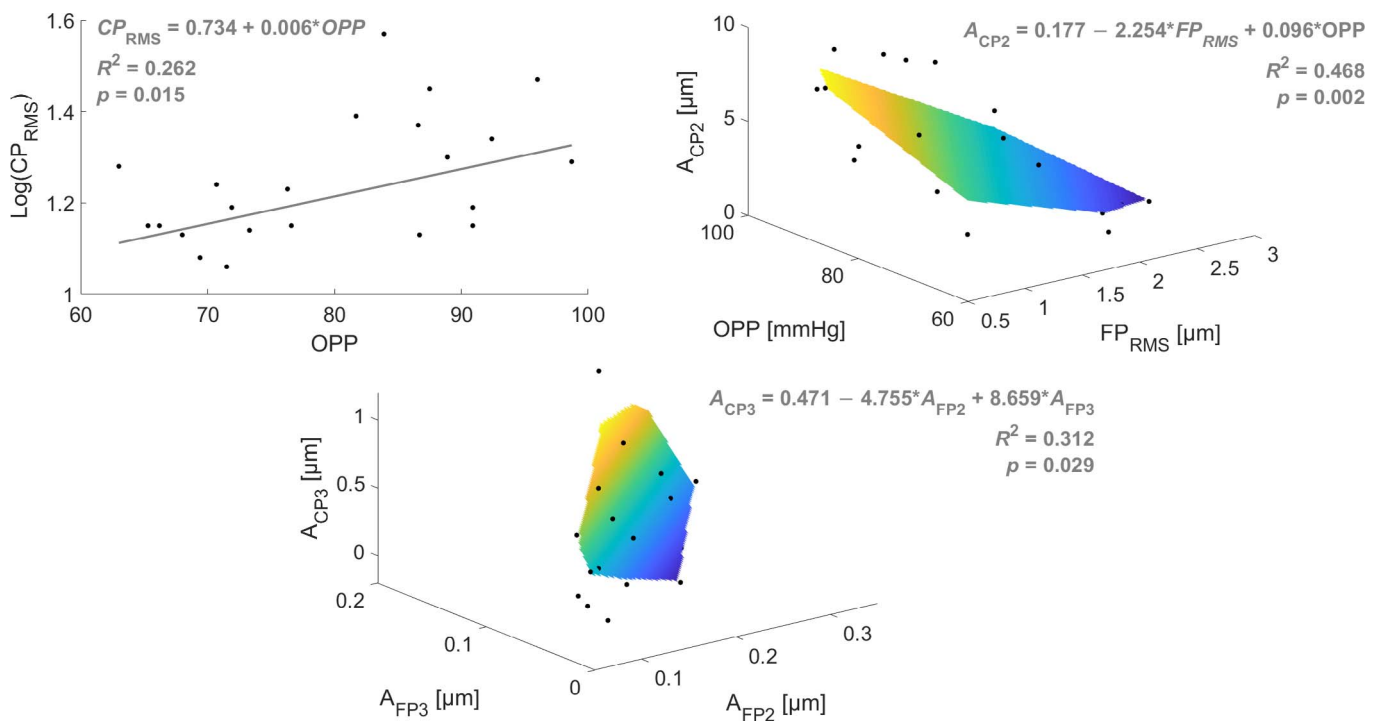


**Figure 6.** Backward stepwise regression models of statistical significance (see Table 3) for CP parameters ( $CP_{RMS}$ ,  $A_{CP2}$ , and  $A_{CP3}$ ) versus FP signal parameters and  $OPP$ .

explained yet. However, based on several studies concerning higher ocular stiffness in glaucomatous eyes<sup>2,55–57</sup> and in normal, ageing eyes,<sup>58</sup> it can be speculated that higher ocular stiffness may contribute to ODP incidence. In our study, linear models revealed that time and spectral parameters of the FP signal and OPP are predictors for amplitudes of the higher CP harmonics,  $A_{CP2}$  and  $A_{CP3}$ . This indicates that, besides the biomechanical properties of the cornea as shown in an animal model,<sup>47</sup> vascular components also influence higher CP harmonics at normal IOP values, leading to changes in the CP morphology. With that, our proposed approach for measurement of both CP and FP signal might help for a better understanding of the mechanism of the ODP formation.

Spectral analysis of CP signal has recently been extended to POAG patients after canaloplasty (Danielewska ME, et al. *IOVS*. 2019;60:ARVO E-Abstract 6202). A decrease in  $A_{CP1}$  and an increase in  $A_{CP3}$ , corresponding to an increase in IOP values, have been noticed between the pre- and post washout from antiglaucoma medications. Also, after the surgery,  $A_{CP3}$  has reached the highest value at 3 months' postoperatively, most likely reflecting alterations in corneal stiffness caused by the surgery. Those findings emphasize the significance of the CP characteristic in monitoring glaucomatous eyes after surgeries aiming at IOP reduction. The relationship between the CP signal and the FP signal, as proposed in this study, can be a more valuable factor in clinical practice than the CP signal alone. It further has the potential to indirectly monitor not only biomechanical but also vascular postoperative alterations caused by ocular surgeries.

The cornea pulsates synchronously to the cardiac rhythm, as indicated by the fact that the CP signal parameters were shown to be highly correlated with cardiovascular activity.<sup>18,22</sup> Furthermore, it has to be noted that the pressure within the choroid is a determinant of the pressure-volume relationship.<sup>59,60</sup> In our study, the systemic BP indirectly influences, by means of the FP and OPP, the amplitudes of the second and third CP harmonics. These findings underline the role of FP and OPP in the generation of the CP signal characteristics.

The partial correlation analysis, independently controlled by age, sex, or HR, showed that the energy of the CP signal, expressed by  $CP_{RMS}$ , is correlated with BP parameters and OPP. The amplitude of the second CP harmonic is highly correlated with the parameters of the FP signal and OPP, after correcting

for age or sex. Interestingly, sex-controlled relationships between the  $CP_{RMS}$ ,  $A_{CP2}$ , and all of the FP signal parameters are the most significant in this study. Changes in ocular circulation are influenced by sex and physiological changes in sex hormone levels, apart from age and other individual ocular and systemic variables.<sup>41,61,62</sup> Since all women participating in this study were in a premenopausal age, potential variability in choroidal blood flow caused by sex hormones can influence the CP time course and the character of its relationship to the FP, when sex is not controlled for. It is evident that vascular components have an impact on the CP signal morphology; however, subject's age and sex should be taken into account.

One limitation of this study is the assumption of a linear model in assessing the relationship between the CP and FP signals. However, despite its simplicity, it allows to explain the fundamental relationship between anterior and posterior eye pulsations. To explain whether the amplitude of the second harmonic is associated with eye movements or the tissues biomechanics, future studies based on an animal model with strictly controlled ocular biomechanical parameters are needed.

Summarizing, our study in healthy subjects showed that both changes in the parameters of the FP signal and in OPP values have an impact on time and spectral characteristics of the CP signal. The proposed linear time invariant model revealed that the eye globe transfers information between signals of the posterior and the anterior eye, relatively amplifying higher spectral harmonics. The variations of the CP morphology are correlated with the fundus pulsation and OPP. Thus, investigation of changes in corneal pulsation parameters, in relation to cardiovascular activity signals, might help with gaining new insights into the nature of the eye dynamics and the pathophysiology of eye diseases.

## Acknowledgments

The authors thank Katarzyna J. Witkowska and Piotr Woźniak for their support in ophthalmic examination of the subjects, D. Robert Iskander for his fruitful comments on an earlier version of the manuscript, and Cezary Sielużycki for proofreading.

MED and MMP acknowledge the support of the statutory funds of Wrocław University of Science and Technology.

Disclosure: **M.E. Danielewska**, None; **A. Messner**, None; **R.M. Werkmeister**, None; **M.M. Placek**, None; **V. Aranha dos Santos**, None; **M. Rękas**, None; **L. Schmetterer**, None

## References

- Evans DW, Hosking SL, Embleton SJ, Morgan AJ, Bartlett JD. Spectral content of the intraocular pressure pulse wave: glaucoma patients versus normal subjects. *Graefes Arch Clin Exp Ophthalmol*. 2002;240:475–480.
- Hommer A, Fuchsjäger-Mayrl G, Resch H, Vass C, Garhofer G, Schmetterer L. Estimation of ocular rigidity based on measurement of pulse amplitude using pneumotometry and fundus pulse using laser interferometry in glaucoma. *Invest Ophthalmol Vis Sci*. 2008;49:4046–4050.
- Dion C, Singh K, Ozaki T, Lesk MR, Costantino S. Analysis of pulsatile retinal movements by spectral-domain low-coherence interferometry: influence of age and glaucoma on the pulse wave. *PLoS One*. 2013;8:e54207.
- Danielewska ME, Krzyżanowska P, Iskander DR. Glaucomatous and age-related changes in corneal pulsation shape. The ocular dicrotism. *PLoS One*. 2014;9:e102814.
- Stalmans I, Harris A, Vanbellinghen V, Zeyen T, Siesky B. Ocular pulse amplitude in normal tension and primary open angle glaucoma. *J Glaucoma*. 2008;17:403–407.
- Schmetterer L, Salomon A, Rheinberger A, Unfried C, Lexer F, Wolzt M. Fundus pulsation measurements in diabetic retinopathy. *Graefes Arch Clin Exp Ophthalmol*. 1997;235:283–287.
- Savage HI, Hendrix JW, Peterson DC, Young H, Wilkinson CP. Differences in pulsatile ocular blood flow among three classifications of diabetic retinopathy. *Invest Ophthalmol Vis Sci*. 2004;45:4504–4509.
- Schmetterer L, Kruger A, Findl O, Breiteneder H, Eichler HG, Wolzt M. Topical fundus pulsation measurements in age-related macular degeneration. *Graefes Arch Clin Exp Ophthalmol*. 1998;236:160–163.
- Mori F. Pulsatile ocular blood flow study: decreases in exudative age related macular degeneration. *Br J Ophthalmol*. 2001;85:531–533.
- Zuckerman JL, Taylor KD, Grossman HJ. Noncontact detection of ocular pulse-correlation with carotid stenosis. *Invest Ophthalmol Vis Sci*. 1977;16:1018–1024.
- Knecht PB, Menghini M, Bachmann LM, Baumgartner RW, Landau K. The ocular pulse amplitude as a noninvasive parameter for carotid artery stenosis screening: a test accuracy study. *Ophthalmology*. 2012;119:1244–1249.
- Schmidt KG, von Rückmann A, Kemkes-Matthes B, Hammes HP. Ocular pulse amplitude in diabetes mellitus. *Br J Ophthalmol*. 2000;84:1282–1284.
- Dimitrova G, Kato S, Tamaki Y, et al. Choroidal circulation in diabetic patients. *Eye*. 2001;15:602–607.
- Rękas M, Danielewska ME, Byszewska A, et al. Assessing efficacy of canaloplasty using continuous 24-hour monitoring of ocular dimensional changes. *Invest Ophthalmol Vis Sci*. 2016;57:2533–2542.
- Silver DM, Farrell RA, Langham ME, O'Brien V, Schilder P. Estimation of pulsatile ocular blood flow from intraocular pressure. *Acta Ophthalmol*. 1989;67:25–29.
- Ramos RF, Stamer WD. Effects of cyclic intraocular pressure on conventional outflow facility. *Invest Ophthalmol Vis Sci*. 2008;49:275–281.
- Trew DR, James CB, Thomas SHL, Sutton R, Smith SE. Factors influencing the ocular pulse — the heart rate. *Graefes Arch Clin Exp Ophthalmol*. 1991;229:553–556.
- Kasprzak HT, Iskander DR. Spectral characteristics of longitudinal corneal apex velocities and their relation to the cardiopulmonary system. *Eye (Lond)*. 2007;21:1212–1219.
- Danielewska ME, Iskander DR, Kowalska M, Kasprzak HT. Phase dependencies between longitudinal corneal apex displacement and cardiovascular signals: is the ocular pulse influenced by the electrical activity of the heart? *Clin Exp Optom*. 2012;95:631–637.
- Schmetterer LF, Lexer F, Unfried CJ, Sattmann H, Fercher AF. Topical measurement of fundus pulsations. *Opt Eng*. 1995;34:711–717.
- Iskander DR, Kasprzak HT. Dynamics in longitudinal eye movements and corneal shape. *Ophthalmic Physiol Opt*. 2006;26:572–579.
- Kowalska MA, Kasprzak HT, Iskander DR, Danielewska M, Mas D. Ultrasonic in vivo measurement of ocular surface expansion. *IEEE Trans Biomed Eng*. 2011;58:674–680.
- Singh K, Dion C, Wajszilber M, Ozaki T, Lesk MR, Costantino S. Measurement of ocular fundus pulsation in healthy subjects using a novel



- Fourier-domain optical coherence tomography. *Invest Ophthalmol Vis Sci.* 2011;52:8927–8932.
24. Dragostinoff N, Werkmeister RM, Klaizer J, Gröschl M, Schmetterer L. Time course and topographic distribution of ocular fundus pulsation measured by low-coherence tissue interferometry. *J Biomed Opt.* 2013;18:121502.
  25. Kaufmann C, Bachmann LM, Robert YC, Thiel MA. Ocular pulse amplitude in healthy subjects as measured by dynamic contour tonometry. *Arch Ophthalmol.* 2006;124:1104–1108.
  26. Asejczyk-Widlicka M, Krzyżanowska-Berkowska P, Kowalska M, Iskander DR. Clinical utility of spectral analysis of intraocular pressure pulse wave. *BMC Ophthalmol.* 2014;14:30.
  27. Vulsteke C, Stalmans I, Fieuws S, Zeyen T. Correlation between ocular pulse amplitude measured by dynamic contour tonometer and visual field defects. *Graefes Arch Clin Exp Ophthalmol.* 2008;246:559–565.
  28. James CB, Smith SE. Pulsatile ocular blood flow in patients with low tension glaucoma. *Br J Ophthalmol.* 1991;75:466–470.
  29. Fontana L, Poinosawmy D, Bunce CV, O'Brien C, Hitchings RA. Pulsatile ocular blood flow investigation in asymmetric normal tension glaucoma and normal subjects. *Br J Ophthalmol.* 1998;82:731–736.
  30. Singh K, Dion C, Costantino S, Wajszilber M, Lesk MR, Ozaki T. Development of a novel instrument to measure the pulsatile movement of ocular tissues. *Exp Eye Res.* 2010;91:63–68.
  31. Dragostinoff N, Werkmeister RM, Gröschl M, Schmetterer L. Depth-resolved measurement of ocular fundus pulsations by low-coherence tissue interferometry. *J Biomed Opt.* 2009;14:054047.
  32. Augustin M, Fialová S, Fischak C, Schmetterer L, Hitzenberger CK, Baumann B. Ocular fundus pulsations within the posterior rat eye: choriocleral motion and response to elevated intraocular pressure. *Sci Rep.* 2017;7:8780.
  33. Kowalska MA, Kasprzak HT, Robert Iskander D. Comparison of high-speed videokeratometry and ultrasound distance sensing for measuring the longitudinal corneal apex movements. *Ophthalmic Physiol Opt.* 2009;29:227–234.
  34. Licznarski TJ, Jaroński J, Kosz D. Ultrasonic system for accurate distance measurement in the air. *Ultrasonics.* 2011;51:960–965.
  35. ANSI Z136.1-2014, *American National Standard for Safe Use of Lasers.* Laser Institute of America, Orlando, Florida, 2014.
  36. IEC 60825-1:2014, *Safety of laser products - Part 1: Equipment classification and requirements,* International Electrotechnical Commission, Geneva, Switzerland, 2014.
  37. Dallinger S, Findl O, Strenn K, Eichler H-G, Wolzt M, Schmetterer L. Age dependence of choroidal blood flow. *J Am Geriatr Soc.* 1998;46:484–487.
  38. Armstrong RA. When to use the Bonferroni correction. *Ophthalmic Physiol Opt.* 2014;34:502–508.
  39. Ravalico G, Toffoli G, Pastori G, Crocè M, Calderini S. Age-related ocular blood flow changes. *Invest Ophthalmol Vis Sci.* 1996;37:2645–2650.
  40. Lam AKC, Chan S-T, Chan H, Chan B. The effect of age on ocular blood supply determined by pulsatile ocular blood flow and color Doppler ultrasonography. *Optom Vis Sci.* 2003;80:305–311.
  41. Centofanti M, Bonini S, Manni G, Guinetti-Neuschüler C, Bucci MG, Harris A. Do sex and hormonal status influence choroidal circulation? *Br J Ophthalmol.* 2000;84:786–787.
  42. Schmidl D, Schmetterer L, Garhöfer G, Popa-Cherecheanu A. Gender differences in ocular blood flow. *Curr Eye Res.* 2015;40:201–212.
  43. Božić M, Dukić ML, Stojković M. Spectral analysis of intraocular pressure pulse wave in open angle glaucomas and healthy eyes. *Curr Eye Res.* 2012;37:1019–1024.
  44. Charman WN, Heron G. Microfluctuations in accommodation: an update on their characteristics and possible role. *Ophthalmic Physiol Opt.* 2015;35:476–499.
  45. Bartuzel MM, Iskander DR, Marin-Franch I, Lopez-Gil N. Defocus vibrations in optical systems – considerations in reference to the human eye. *J Opt Soc Am A.* 2019;36:464–470.
  46. Schmetterer L, Dallinger S, Findl O, Eichler HG, Wolzt M. A comparison between laser interferometric measurement of fundus pulsation and pneumotonometric measurement of pulsatile ocular blood flow. 1. Baseline considerations. *Eye.* 2000;14:39–45.
  47. Rogala MM, Danielewska ME, Antończyk A, et al. In-vivo corneal pulsation in relation to in-vivo intraocular pressure and corneal biomechanics assessed in-vitro. An animal pilot study. *Exp Eye Res.* 2017;162:27–36.
  48. Davies PF, Tripathi SC. Mechanical stress mechanisms and the cell. An endothelial paradigm. *Circ Res.* 1993;72:239–245.
  49. Matthews BD, Overby DR, Mannix R, Ingber DE. Cellular adaptation to mechanical stress: role

- of integrins, Rho, cytoskeletal tension and mechanosensitive ion channels. *J Cell Sci.* 2006; 119(pt 3):508–518.
50. Coleman DJ, Trokel S. Direct-recorded intraocular pressure variations in a human subject. *Arch Ophthalmol.* 1969;82(5):637–640.
  51. Tamm ER. The role of the ciliary body in aqueous humor dynamics: structural aspects. In: Besharse J, Dana R, Dartt D, eds. *Encyclopedia of the Eye.* Oxford, UK: Elsevier Ltd. 2009:179–186.
  52. Tamm ER. The trabecular meshwork outflow pathways: structural and functional aspects. *Exp Eye Res.* 2009;88:648–655.
  53. Kiel JW, Hollingsworth M, Rao R, Chen M, Reitsamer HA. Ciliary blood flow and aqueous humor production. *Prog Retin Eye Res.* 2011;30: 1–17.
  54. Danielewska ME, Iskander DR, Krzyzanowska-Berkowska P. Age-related changes in corneal pulsation: ocular dicrotism. *Optom Vis Sci.* 2014; 91:54–59.
  55. Ebneter A, Wagels B, Zinkernagel MS. Non-invasive biometric assessment of ocular rigidity in glaucoma patients and controls. *Eye.* 2009;23: 606–611.
  56. Dastiridou AI, Ginis H, Tsilimbaris M, et al. Ocular rigidity, ocular pulse amplitude, and pulsatile ocular blood flow: the effect of axial length. *Invest Ophthalmol Vis Sci.* 2013;54:2087–2092.
  57. Coudrillier B, Tian J, Alexander S, Myers KM, Quigley HA, Nguyen TD. Biomechanics of the human posterior sclera: age- and glaucoma-related changes measured using inflation testing. *Invest Ophthalmol Vis Sci.* 2012;53:1714–1728.
  58. Pallikaris IG, Kymionis GD, Ginis HS, Kounis GA, Tsilimbaris MK. Ocular rigidity in living human eyes. *Invest Ophthalmol Vis Sci.* 2005;46: 409–414.
  59. Kiel JW. The effect of arterial pressure on the ocular pressure-volume relationship in the rabbit. *Exp Eye Res.* 1995;60:267–278.
  60. Bayerle-Eder M, Kolodjaschna J, Wolzt M, Polska E, Gasic S, Schmetterer L. Effect of a nifedipine induced reduction in blood pressure on the association between ocular pulse amplitude and ocular fundus pulsation amplitude in systemic hypertension. *Br J Ophthalmol.* 2005;89: 704–708.
  61. Centofanti M, Zarfati D, Manni GL, et al. The influence of oestrogen on the pulsatile ocular blood flow. *Acta Ophthalmol Scand.* 2000;78:38–39.
  62. Kavroulaki D, Gugleta K, Kochkorov A, Katamay R, Flammer J, Orgul S. Influence of gender and menopausal status on peripheral and choroidal circulation. *Acta Ophthalmol.* 2010;88:850–853.